Unique Dynamical Approach of Fully Wrapping Dendrimer-like Soft Nanoparticles by Lipid Bilayer Membrane

Ruohai Guo, Jian Mao, and Li-Tang Yan*

Key Laboratory of Advanced Materials (MOE), Department of Chemical Engineering, Tsinghua University, Beijing 100084, P. R. China

ABSTRACT Wrapping dendrimer-like soft nanoparticles by cell membrane is an essential event in their endocytosis in drug and gene delivery, but this process remains poorly elucidated. Using computer simulations and theoretical analysis, we report the detailed dynamics of the process in which a lipid bilayer membrane fully wraps a dendrimer-like soft nanoparticle. By constructing a phase diagram, we firstly demonstrate that there exist three states in the interaction between a dendrimer and a lipid bilayer membrane, *i.e.*, penetration, penetration and partial wrapping, and full wrapping states. The wrapping process of dendrimer-like nanoparticles is found to take a unique approach where the penetration of the dendrimer into the membrane plays a significant role. The analysis of various energies within the system provides a theoretical justification to the state transition observed from simulations. The findings also support recent experimental results and provide a theoretical explanation for them. We expect that these findings are of immediate interest to the study of the cellular uptake of dendrimer-like soft nanoparticles and can prompt the further application of this class of nanoparticles in nanomedicine.

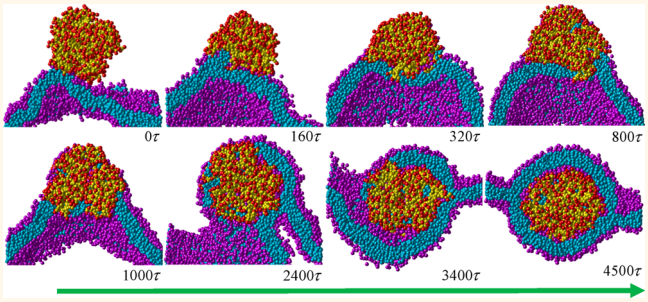

KEYWORDS: lipid membrane · soft nanoparticles · wrapping process · dynamical approach · dendrimer · computer simulation

The use of dendrimer-like soft nanoparticles in biomedicine and nanotechnology is rapidly increasing, and there have been a large number of studies aimed at examining and understanding the cellular uptake of these nanoparticles.[1−5] Upon the unique molecular topology, extended range of dendrimer-like nanoparticles can include not only dendrimers but also some hyperbranched macromolecules as well as general nanoparticles with long tethers.[1,2] Understanding the transmembrane transport mechanisms of this class of nanoparticles is of essential importance to their applications. However, in contrast to general "hard" nanoparticles, the elastic deformation and complicated molecular topology of dendrimer-like soft nanoparticles may strongly affect their interaction with cell membrane.[6]

Recently, experimental[1,2,7,8] and theoretical[3−5,9−13] studies have demonstrated that the transmembrane transport of dendrimerlike nanoparticles can take the mechanisms of membrane disruption, penetration, and endocytosis, depending on different physicochemical parameters. Although the first two mechanisms have been extensively explored, the molecular-scale details of the endocytosis of this class of nanoparticles have remained to be definitely elucidated. One particular aspect of the problem that has not been addressed and could be of great relevance, concerns the interplay between two different mechanisms, *e.g.*, penetration and endocytosis. Understanding how the penetration of dendrimer-like nanoparticles affects their endocytosis process in the molecular scale is related to the fundamental biological responses and cytotoxicity, and is thereby one critical issue to be resolved for their further applications in nanomedicine. Experimentally, it requires direct measurements in single cell and is thus very difficult and more challenging.[2]

* Address correspondence to ltyan@mail.tsinghua.edu.cn.

Received for review June 30, 2013 and accepted November 20, 2013.

Published online November 20, 2013
10.1021/nn4033344

Here, we present the first study on the detailed dynamics of the process where a lipid bilayer membrane fully wraps a dendrimer by employing large-scale computer simulations. Notably, the penetration of the dendrimer-like nanoparticle into the membrane is found to play a crucial role in this wrapping process, demonstrating a unique dynamical approach. In particular, we identify a state transition from penetration to full wrapping during the transmembrane transport of this class of nanoparticles. The energetic analysis provides a theoretical justification to the simulation results. Some recent experimental findings can also be rationalized by the simulations and theoretical analysis.

Full technical details on the simulation method and the models of lipid and dendrimer are described in the Method section. Briefly, the dissipative particle dynamics (DPD) technique is used in the simulations which extends the simulation scales of time and space to be appropriate to the study of nanoparticle-membrane systems with explicit water.[14−16] An effective coarse-grained methodology of dendrimers is used in the modeling, which has been proved its validity and efficiency in the simulations of their conformational behaviors and interactions with lipid bilayers (see refs 12 and 13, and Table S1). The model of the dendrimer-like nanoparticle is mapped from the poly(amidoamine) (PAMAM) like dendrimer.[2,12,13] Only the terminal beads of the dendrimer model are hydrophilic while the other moiety of the dendrimer is hydrophobic. Each amphiphilic lipid consists of a headgroup and two tails. The headgroup contains three connected hydrophilic beads. Each tail includes three connected hydrophobic beads. To mimic a real cell membrane with a larger area-to-volume ratio, here we use *N*-varied DPD method where the targeted membrane tension can be maintained.[17] This technique facilitates the control of the membrane tension through offering sufficient excess area to release the extra tension induced by a large membrane deformation due to the wrapping. Figure 1 shows the plot of the surface tension, σ, as a function of area per lipid, A_l, for the lipid membranes used in the present simulations. The threshold of the lipid density corresponding to zero tension is observed at about $A_l \approx 1.28 r_c^2$ ($r_c \approx$ 0.7 nm is the length unit of the simulations). Before this point, the membrane has a negative surface tension where the lipid compression is required to balance the energy cost of membrane buckling. In a real cell, the negative surface tension can be generated by the cytoskeleton, dynamin or actin filaments.[18−20]

RESULTS AND DISCUSSION

For the initial simulations, a dendrimer is initially positioned in close proximity above the surface of a membrane. To determine the mechanisms of the transmembrane transport of dendrimers, we performed 66

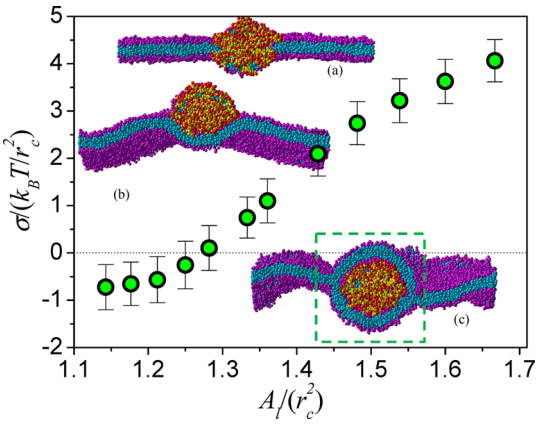

Figure 1. Calculated surface tension of lipid membranes, σ, as a function of area per lipid, A_l. Error bars represent the standard deviation. The representative snapshots show three typical phases of the seventh generation (G7) dendrimers interacting with a lipid bilayer membrane at different surface tensions, σ: (a) penetration at $\sigma = 2.09\ k_BT/r_c^2$, (b) penetration and partial wrapping at $\sigma = 0.10\ k_BT/r_c^2$, and (c) full wrapping at $\sigma = -0.72\ k_BT/r_c^2$. Solvent beads and counterions are not shown for clarity. Color scheme: lipid head beads (pink), lipid tail beads (cyan), charged beads of dendrimer (red), and uncharged beads of dendrimer (yellow).

simulations (35 μs each) for membranes with σ changing from $-0.72\ k_BT/r_c^2$ to $4.06\ k_BT/r_c^2$ and dendrimer generation varying from 3 to 8. We find that membrane disruption can be induced for all dendrimers when σ is larger than $2.09\ k_BT/r_c^2$. Consideration of the details of the membrane disruption is beyond the scope of the present study and can be found elsewhere.[2,7−13] Instead, we focus on the penetration and wrapping behaviors where $\sigma \leq 2.09 k_BT/r_c^2$. The snapshots in Figure 1 and Supporting Information videos show the typical equilibrium states where the seventh dendrimer (G7) is used as a sample. For relatively high surface tension at $\sigma = 2.09 k_BT/r_c^2$, a penetration state is observed, where dendrimer beads insert into the membrane and lead to small pores in it (Figure 1a and Supporting Information Video 1). Such high surface tension can enhance the penetration of dendrimer beads across the tense membrane.[12] In this case, we note that wrapping however does not happen. As surface tension decreases to near zero point, the penetration of dendrimer beads across the tensionless membrane is significantly reduced (Figure 1b and Supporting Information Video 2). Instead the dendrimer is partially wrapped by the membrane. There exist a penetration state and a partial wrapping state for the tensionless membrane, in agreement with some previous simulations.[4,9] With further decreasing σ to $-0.72\ k_BT/r_c^2$, the state becomes full wrapping, where the dendrimer is completely wrapped by the membrane, resulting in a dendrimer-encased vesicle (Figure 1c and Supporting Information Video 3). The formation of the full wrapping state plays a crucial role in the endocytosis of the dendrimer. Little has reported

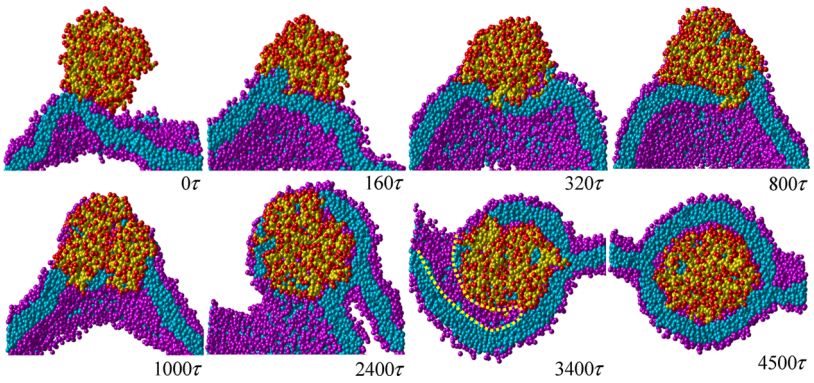

Figure 2. The enlarged local structures within the dashed square in Figure 1c show successive stages in a full wrapping process of the G7 dendrimer at $\sigma = -0.72\ k_BT/r_c^2$.

on the formation of this structure in previous simulations. However, a recent experiment of Kelly *et al.*[21] of the stoichiometry of the PAMAM dendrimer–phospholipid interactions suggested the presence of the dendrimer-encased vesicle. The details of this structure are difficult to experimentally demonstrate,[2] and its formation mechanism has not been examined in the molecular scale.

To address these concerns, here we provide a detailed insight into its formation dynamics. For this purpose, the successive evolution of local structure as marked by the dashed square in Figure 1c is presented in Figure 2 that illustrates the dynamical approach of the full wrapping state in the molecular scale. A more detailed dynamical process can also be found in Supporting Information Video 3. It is interesting to see that the evolution process can be divided into two stages, with the boundary at about 1000τ ($\tau \approx 7.7$ ns is the time unit of the simulations). In the first stage, the dendrimer is attracted to the membrane and tends to deform along the membrane surface (320τ). Simultaneously, some lipid molecules around the dendrimer are pulled away from the membrane and then insert into the dendrimer (800τ). This activated process is driven mainly by the strong attraction between the dendrimer hydrophobic moiety and the hydrophobic lipid tails.[7,10] The unique molecular topology of the dendrimer provides inner space for the insertion of lipids into it. At about 1000τ, a complex comprised of dendrimer and lipids forms, resembling the penetration state of a dendrimer across a tensionless membrane. Clearly, the dendrimer penetration dominates the first stage of the process. In the following stage, we however find a state transition from penetration to full wrapping, which is different with the systems of tensionless or tensed membrane with positive surface tension and has not been reported previously.[3–5,9–13] In particular, the lipid–dendrimer complex, with almost isotropic shape, behaves as a larger "particle" from 1000τ. The membrane with negative surface tension significantly bends around the complex particle (2400τ). As a result, the membrane close to the

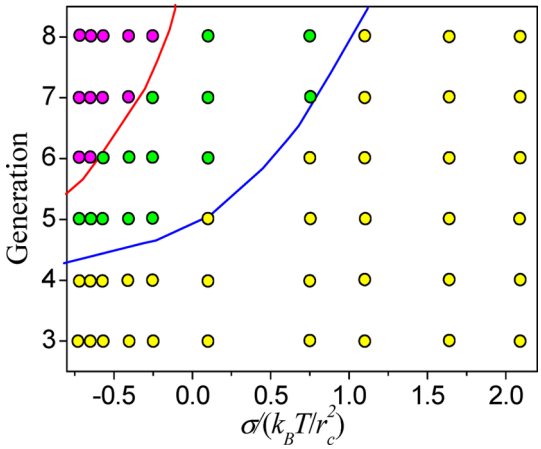

Figure 3. A phase diagram from simulations, describing the states as a function of dendrimer generation and membrane tension σ. The yellow, green, and pink circles denote penetration (no wrapping), penetration (no wrapping) and partial wrapping, and full wrapping states, respectively. The boundaries are indicated by the red and blue lines for clarity only.

complex particle is locally deformed and a local membrane curvature is created. At 3400τ, the complex particle is gradually wrapped by the membrane, along with local membrane fusion (as denoted by the yellow dashed curve), and moves downward consequently. Finally, the complex is entirely wrapped by the membrane. Note in real cellular endocytosis, the fully wrapped object can be further internalized through membrane fission accelerated by external force, *e.g.*, actin polymerization or Sar1.[18–20] The two stages demonstrated in Figure 2 reveal that there may be a cooperative behavior of two basic mechanisms, *i.e.*, penetration and endocytosis, in the cellular uptake of a dendrimer-like nanoparticle.

To evaluate the generality of this unique dynamical approach, we systematically simulate the states in the cellular uptake of dendrimer-like nanoparticles as a function of dendrimer generation and membrane tension, which allow us to construct a phase diagram in the two-parameter space, as shown in Figure 3. Three characteristic regions separated by two boundaries

can be identified in the phase diagram. Indeed, there exists a region where the dendrimer can be fully wrapped by the membrane and the dendrimer penetration plays a significant role in it (*e.g.*, Figure 1c). As denoted by the pink circles, the region of the full wrapping state ranges with dendrimer generation no less than 6 and σ no larger than $-0.25\ k_BT/r_c^2$. Increasing membrane tension or decreasing dendrimer generation leads to the coexisting state of penetration and partial wrapping, as marked by the green circles (*e.g.*, Figure 1b). For smaller dendrimers and higher values of σ, the wrapping cannot happen and the structure of dendrimer–lipid complex remains, the state being only penetration (Figure 1a). These simulation results definitely demonstrate that the state transition in the cellular uptake of dendrimer-like nanoparticles strongly depends on membrane tension and particle size. Particularly, the negative surface tension of membrane, that is usual in the real cellular system,[17−20] is a key factor to trigger the state transition, since it can enhance the curvature and fluctuation of the membrane so that the motion of the complex cannot be "restricted" too much and can behave as a big "particle" to be wrapped.

To understand the role of dendrimer penetration in the following wrapping, we calculate the asphericity, A_s, and the radius of gyration, R_g, of dendrimer. Here A_s is calculated from the gyration tensor of all dendrimer beads, and a higher A_s corresponds to a higher anisotropic shape.[22] Figure 4 and inset show the evolution of A_s and the σ-dependence of equilibrium R_g for a G7 dendrimer interacting with a membrane. The figure demonstrates that for all values of σ the dendrimer presents anisotropic shape first and then turns to be isotropic. Interestingly, we find that a membrane with lower σ corresponds to a dendrimer with more isotropic shape and larger size at equilibrium. In particular, given that the R_g of a G7 dendrimer is about $5.73r_c$, the dendrimer size increases by about 12% at $\sigma = -0.72\ k_BT/r_c^2$. The formation of the lipid–dendrimer complex accounts for these changes of the dendrimer. Previous theoretical study indicated that the full wrapping of a soft nanoparticle can be suppressed due to its elastic deformation.[6] Our simulations demonstrate that the deformation of dendrimer is significantly reduced when a lipid–dendrimer complex forms during the penetration of dendrimer, providing an advantageous factor for its full wrapping. It has also been experimentally[23] and theoretically[16] revealed that a spherical nanoparticle is easier to be internalized through endocytosis. As demonstrated in Figures 2 and 4, the complex holds a more uniformly spherical shape especially at a lower σ, benefitting its following wrapping. The size increase of the complex is another advantageous factor for its full wrapping, because wrapping a small particle usually extremely raises the bending energy of the membrane.[24,25] Taken together,

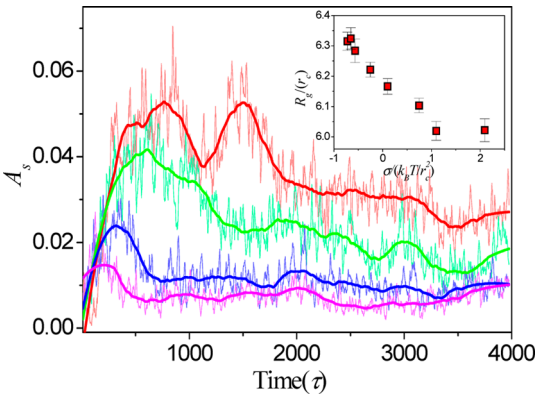

Figure 4. Time evolution of the asphericity A_s of a G7 dendrimer interacting with a membrane at different σ. Color scheme: (red) $\sigma = 2.09\ k_BT/r_c^2$, (green) $\sigma = 1.10\ k_BT/r_c^2$, (blue) $\sigma = 0.75\ k_BT/r_c^2$, and (pink) $\sigma = -0.72\ k_BT/r_c^2$. The inset shows the radius of gyration R_g of the dendrimer as a function of σ.

the penetration of dendrimer in the first stage, inducing the formation of dendrimer–lipid complex, can greatly facilitates the full wrapping in the second stage of the dynamical approach.

To gain more detailed insight into the facilitating effect of dendrimer penetration on its full wrapping, we provide a quantitative analysis for the energy of the system based on the Canham-Helfrich theory.[26,27] The details of this analysis can be found in the Method section. Briefly, upon interaction between a dendrimer and a lipid membrane, the contact energy drives the local wrapping of the membrane around the dendrimer which, however, is opposed by the bending energy of the membrane. The wrapping is also influenced by the tension energy that is usually induced by the excess membrane pulled toward the wrapping site.[27] The total energy of the system E is thereby an equation of these three items (see eq 2). E with respect to the wrapping degree of the dendrimer by the membrane, f_w, can be found by minimizing the equation. With increasing f_w from 0 to 1, the equilibrium wrapping state can be obtained, where E reaches a local extremum.[6]

Figure 5 and its inset show E as a function of f_w for the G7 dendrimer at three values of σ. At $\sigma = 1.10\ k_BT/r_c^2$, E increases monotonically with f_w, where the high positive tension energy dominates the wrapping process and the wrapping is inhibited. When σ decreases to $0.10\ k_BT/r_c^2$, a locally minimum occurs at $f_w \approx 0.12$, as denoted by the circle in the inset. This energy extremum indicates the presence of a metastable partial wrapping state in addition to the no wrapping state. For the same dendrimer in a system without membrane, its equilibrated R_g is reduced to about $5.73r_c$. If the dendriemer with this size interacts with a membrane at the same σ, there however exists only no wrapping state (dashed green line), revealing again that the penetration of dendrimer can facilitate wrapping process through modifying its shape and size. With further deceasing σ to $-0.57\ k_BT/r_c^2$, the energy

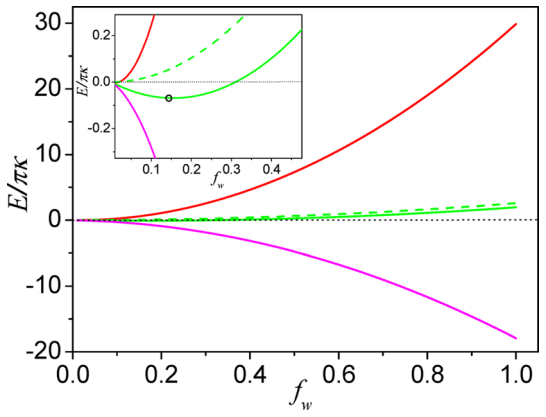

Figure 5. The energy of the system, *E*, as a membrane wraps around a G7 dendrimer with wrapping degree, f_w, for σ = 1.10 k_BT/r_c^2 (red), 0.10 k_BT/r_c^2 (green), and −0.57 k_BT/r_c^2 (pink). The green dashed line represents the plot for a particle with $R_g = 5.73r_c$. κ is the elastic module of the membrane with unit of energy k_BT.

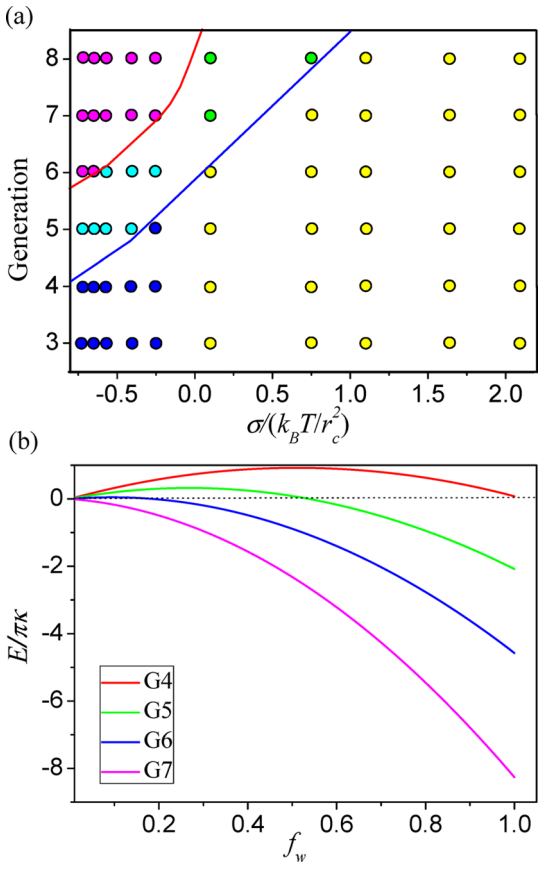

Figure 6. (a) The phase diagram from quantitative analysis of system energy, describing the states as a function of dendrimer generation and membrane tension σ. The yellow, green, and pink circles denote penetration (no wrapping), penetration (no wrapping) and partial wrapping, and full wrapping states, respectively. The cyan circles represent the case having a metastable state of partial wrapping and a stable state of full wrapping while the blue circles represent the case having a stable state of no wrapping and a metastable state of partial or full wrapping. Phase boundaries are indicated by the red and blue lines for clarity only. (b) The $E-f_w$ plots as a membrane wraps around different dendrimers at σ = −0.25 k_BT/r_c^2.

barrier vanishes and the full wrapping state becomes the only stable state. By comparing these theoretical results with the corresponding simulation results in the phase diagram of Figure 3, it is interesting to find that the energetic analysis is consistent with the simulations. We further calculate the energetic equilibrium states of all the points in Figure 3, allowing us to construct a phase diagram based on the energetic analysis. Figure 6a shows the phase diagram where, in addition to the three above cases, two different cases occur as marked by the cyan and blue circles, respectively. The $E-f_w$ curves of these points are presented in Figure 6b. One can find that, for the blue circles (*i.e.*, the red and green curves), there exist a local extremum at a no wrapping state with an energy barrier to reach a partial or full wrapping state. For the cyan circles (*i.e.*, the blue curve), the energy barrier almost disappears so that a long platform occurs at the initial stage of the curve corresponding to a metastable state of partial wrapping. This metastable state is followed by the stable state of full wrapping. The blue points could be incorporated into the no wrapping region due to the high barrier in the energy curves while the long platform in the energy curves clarifies that the cyan circles could be included in the region of partial wrapping. Thus, we get the similar state transition boundaries in Figure 6a as with those in Figure 3. This reveals again that the dendrimer−lipid complex behaves as a hard particle due to the deformation restriction exerted by the lipids inserting into the dendrimer. In comparison with the simulations, the energetic analysis provides more detailed information on the metastable state of the system.

The close agreement between energy analysis and simulation much helps us to understand the effects of σ and dendrimer size. A positive σ leads to a positive tension energy E_t that opposes the wrapping process. However, it turns to drive the wrapping process when σ and E_t hold negative values. The full wrapping phase can be induced if σ is negative enough. In a real system, cells can actively control and adjust their membrane tension for the purpose of surface area regulation,[28] so that the negative surface tension can be generated by the cytoskeleton,[18] dynamin[19] or actin filaments.[20] When dendrimers are used as nanocarriers for targeted drug delivery, they get spontaneously wrapped by the membrane. Decreasing membrane tension can significantly prompt this wrapping process. The vertical axis of the phase diagrams indicates that decreasing dendrimer generation can suppress the wrapping process. In this case, the surface area of the dendrimer becomes small, leading to the reduced driving potential for wrapping, *i.e.*, the contacting energy. This is particularly useful for the design of the dendrimer-based nanocarrier, because dendrimer size can be modified when it is conjugated with drug molecules. Note that here the

simulations focus on the systems in water. In a real cellular system, the acid/base environments can influence the interaction between dendrimers and lipid membrane since the protonation level of dendrimers could be altered by changing the solution's acidity. Actually, previous simulations have demonstrated that a lower pH can enhance the adsorption of dendrimers on the negatively charged lipid bilayer.[29] This implies that the contacting energy can be significantly strengthened in response to the decrease of pH which will facilitate the wrapping process. However, at very low pH dendriemrs can even induce a hole formation on the membrane as shown by the previous simulations.[29]

Kelly *et al*.[21] studied the stoichiometry as well as the structure in the PAMAM dendrimer−phospholipid interactions. On the basis of their experimental data of the number of bound lipids and the heat release per amine, they suggested that larger dendrimers can induce the steric restriction of dendrimer deformation on the membrane. They further proposed a dendrimer-encased vesicle model based on these data and pointed out the generation-dependence of this model. In this paper, our simulations provide a theoretical support for their results regarding the formation of the dendrimer-encased vesicle model and present the detailed structure and formation mechanism of it. Further, the phase diagram in Figure 3 also demonstrates that the model has generation-dependence and occurs when the dendrimer generation is no less than 6, in agreement with the experimental conclusions obtained by Kelly *et al*.[21]

CONCLUSIONS

In summary, by employing systematic computer simulations and theoretical analysis, we demonstrate how a lipid bilayer membrane fully wraps a dendrimer-like soft nanoparticle. On the basis of the systematic simulations and energetic analysis, we first construct the phase diagram regarding the states in the interaction between a dendrimer and a lipid bilayer membrane and identify three states from the diagram, *i.e.*, penetration, penetration and partial wrapping, and full wrapping. The cooperative behavior of two basic mechanisms, *i.e.*, penetration and endocytosis, is observed in the transmembrane transport of dendrimer-like soft nanoparticles. A state transition from penetration to full wrapping in this process is found and analyzed at the molecular scale. The role of dendrimer penetration in its following wrapping process is explored. The analysis for various energies within the system reproduces the observation from simulations and gives theoretical justification to the phenomena. We finally demonstrate that the relevant experimental presumption can be rationalized and explained by our simulation and theoretical results. These findings are of immediate interest to the study of the cellular uptake of dendrimer-like soft nanoparticles and can prompt the further application of this class of nanoparticles in nanomedicine.

METHODS

Simulation Details. Computer simulations use DPD technique, and an effective coarse-grained methodology of dendrimers is used in the modeling, which has its validity and efficiency proved in the simulations of their conformational behaviors and interactions with lipid bilayers.[12,13] Here, the model of the dendrimer-like nanoparticle is mapped from the polyamidoamine (PAMAM) like dendrimer. Only the terminal beads of the dendrimer model are hydrophilic and carry the charge of +1. The other moiety of the dendrimer is uncharged and hydrophobic. Each amphiphilic lipid consists of a headgroup and two tails. The headgroup contains three connected hydrophilic beads and the top two of them carry the charges of +1 and −1, respectively. Each tail includes three connected hydrophobic beads. The present simulations are carried out using five different interaction forces between beads, *i.e.*, conservative interaction force F^C, dissipative force F^D, random force F^R, spring force F^S, and electrostatic force F^E. The detailed forms of F^C, F^D and F^R, which can be found elsewhere,[14] are of short-range with a fixed cutoff distance, r_c. In particular, the interaction parameters used in F^C are similar to those provided by the MARTINI force field[30,31] and have been successfully used in our previous works.[12,13] Hookean springs with the potential $U_s(i,i+1) = (1/2)k_s(|r_{i,i+1}| - l_0)^2$ is used to construct dendrimers and lipids, where i, $i+1$ represent connecting beads in the molecules. The spring constant, $k_s = 64$, and unstretched length, $l_0 = 0.5r_c$, are chosen so as to fix the average bond length to a desired value. A three-body potential acting between adjacent bead triples in each tail of lipids and the branches of dendrimer, $U_a(i-1,i,i+1) = k_a[1 - \cos(\varphi - \varphi_0)]$ is selected to model the chain stiffness, where the angle φ is defined by the scalar product of the two bonds connecting beads $i-1$, i, and i, $i+1$.[32] Although this paper does not focus on the charge effects in cellular uptake, the electrostatic interaction among charged beads is included based on a modified particle-particle-particle-mesh (P3M) algorithm in which the electrostatic field is solved by smearing the charges over lattice grid.[33] The simulation box is $60r_c \times 60r_c \times 50r_c$ in size and with periodic boundary condition in all directions, which is large enough to avoid the finite size effects. The time step of $\Delta t = 0.02\ \tau$ is chosen ensuring the accurate temperature control over the simulation system.[34] We choose our basic length and time scales to match the experimentally observed area per dipalmitoyl phosphatidylcholine (DPPC) molecule and the typical diffusion coefficient of lipids.[35] Then, we get $r_c \approx 0.70$ nm and $\tau \approx 7.70$ ns.

To mimic a real cell membrane with a larger area-to-volume ratio, we use *N*-varied DPD method where the targeted membrane tension is maintained by monitoring the lipid number per area, N_l^B.[17] In this method, the boundary region of the membrane plays a role as reservoir of lipids, and N_l^B in the boundary region is kept constant by depletion/addition moves. Simultaneously, a corresponding number of water beads are randomly added and deleted to keep the whole density of the simulation box constant. This technique facilitates the control for the membrane tension through offering sufficient excess area to release the tension induced by a large membrane deformation due to the nanoparticle. Note N_l^B can be easily changed into a more general parameter, the area per lipid, A_l.

Energetic Analysis. The energy calculations are based on the cap model that is a good approach to estimate the relevant energy contributions and has been successfully used in other works (see Figure S2).[27,36,37] It will be first assumed that the membrane remains fluid state in the whole simulations, which facilitates the energy calculation because the membrane shape

is easy to be determined.[25,27] Upon interaction between a dendrimer and a lipid membrane, the contact energy E_a with average density ξ_a drives the local wrapping of the membrane around the dendrimer which, however, is opposed by the bending energy of the membrane E_B. According to the classical Canham-Helfrich theory,[26] the bending energy per unit area will be

$$\xi_b = \frac{1}{2}\kappa(\eta_1+\eta_2-\eta_0)^2+\kappa_G(\eta_1\eta_2) \quad (1)$$

where η_1 and η_2 are the local principal curvatures of the membrane surface, η_0 is the spontaneous curvature of the membrane, and κ and κ_G are elastic moduli with unit of energy k_BT. In the following, $\eta_0 = 0$ is assumed for a symmetric membrane, and the second term in eq 1 is ignored because no topological changes will be considered and periodic boundary condition is used for the membrane without edge.[38,39] The wrapping is also influenced by the tension energy E_t that is usually induced by the excess membrane pulled toward the wrapping site. E_t can be calculated as $E_t = \Delta A_a\sigma$, where ΔA_a is the excess membrane area. If the area of the dendrimer covered by membrane is A_c, summarizing these three energy forms yields the total system energy with the following form:

$$E = \xi_a A_c + \frac{1}{2}\kappa(\eta_1+\eta_2)^2 A_c + \Delta A_a\sigma \quad (2)$$

The detailed forms of A_c and ΔA_a are given in Figure S2 in Supporting Information. Note all the energy quantities are denoted in units of k_BT.

An analysis of thin elastic membrane showed that κ can be estimated as $\kappa = \zeta l^2/48$, where ζ and l are elastic modulus and thickness of the membrane.[40] From a linear fit of the $\sigma-A_l$ curve at low membrane tension, we find $\zeta \approx 22.68\ k_BT/r_c^2$. The membrane thickness can be measured as about $4.6r_c$. Thus, determining both of these parameters leads to $\kappa \approx 10k_BT$ for our system. In the present simulations, when an N-varied DPD method is used, an approximately constant σ can be controlled for each simulation, allowing us to explore the effect of membrane tension conveniently. The density of contact energy ξ_a is difficult to obtain. By testing a series of value, we find that $\xi_a = -0.31\ k_BT/r_c^2$ yields a close agreement between the simulations and the theoretical analysis, which is physically reasonable.[27,35] The contacting energy can be influenced by the electrostatic interaction due to the strong attraction between the positive surface charges of the dendrimer and the negative charges of the lipids. Such charge interactions would enhance the binding of dendrimers on the membrane surface.[25] We note that the dendrimer turns to be isotropic with small deformation at the late stage of each simulation (see Figure 4). Thereby the membrane curvatures η_1 and η_2 are set as $\eta_1 \approx \eta_2 = 1/[R_g + (l/2)]$. Here R_g is the radius of gyration of a dendrimer at equilibrium, and its value in each simulation is given in Table S2. The definition of the wrapping degree, f_w, can be found in Figure S2 in Supporting Information. On the basis of aforementioned values, the total system energy E with respect to f_w can be found by minimizing eq 2. With increasing f_w from 0 to 1, the equilibrium wrapping state can be obtained, where E reaches a local extremum.[6]

Note in Figure 1c, the vesicle-encased dendrimer involves a junction line at which the planar bilayer meets the vesicle membrane. The junction bears a close resemblance to a "trilaterally symmetric void" (TSV) where the free energy per unit can be calculated as $\xi_j = \pi\kappa_m/2R_m$.[41] Here κ_m and R_m are the mean curvature bending modulus and radius of monolayer curvature. Taking $\kappa_m = \kappa/2$ and $R_m = [R_g + (l/2)]$, we obtain the free energy cost of creating the junction is about $0.5\pi\kappa\ k_BT$ regardless of the radius of the vesicle. This energy penalty is too low to modify the full wrapping state of the systems in the present work (see Figure S1 in the Supporting Information for the total energy of the systems with full wrapping state). Thus, this structure can be stable within the time scale of the simulations. Actually, in a real cellular process, the disruption of the junction requires an external interaction, *e.g.*, actin polymerization or Sar1.[18−20] The free energy term due to the linear tension of a pore in the membrane is not included in eq 2 because only very small pore or hole can be induced during the penetration of the dendrimer beads into the membrane.[42] In fact, the "pores" formed here are so small that ascribing them to the "molecular-size metastable defects" is more appropriate.[43] Therefore, they are not pores in a very real sense and have negligible contribution to the tension energy. As pore nucleation is an activated process, the spontaneous formation of pore nuclei in a moderately stretched membrane is even infrequent. For the linear tension of a large enough pore in a lipid membrane, its value can be estimated as the order of 10^{-11} J/m.[44]

Conflict of Interest: The authors declare no competing financial interest.

Supporting Information Available: The additional simulation results and videos. This material is available free of charge *via* the Internet at http://pubs.acs.org.

Acknowledgment. The authors thank Dr. Xiaobo Yu and Prof. Xinghua Shi for helpful discussions. This work is supported by the National Natural Science Foundation of China under Grant Nos. 51273105 and 21174080.

REFERENCES AND NOTES

1. Astruc, D.; Boisselier, E.; Ornelas, C. Dendrimers Designed for Functions: from Physical, Photophysical, and Supramolecular Properties to Applications in Sensing, Catalysis, Molecular Electronics, Photonics, and Nanomedicine. *Chem. Rev.* **2010**, *110*, 1857–1959.
2. Leroueil, P. R.; Hong, S.; Mecke, A.; Baker, J. R.; Orr, B. G.; Holl, M. M. B. Nanoparticle Interaction with Biological Membranes: Does Nanotechnology Present a Janus Face? *Acc Chem. Res.* **2007**, *40*, 335–342.
3. Lee, H.; Larson, R. G. Multiscale Modeling of Dendrimers and Their Interactions with Bilayers and Polyelectrolytes. *Molecules* **2009**, *14*, 423–438.
4. Lee, H.; Larson, R. G. Coarse-Grained Molecular Dynamics Studies of the Concentration and Size Dependence of Fifth- and Seventh-Generation PAMAM Dendrimers on Pore Formation in DMPC Bilayer. *J. Phys. Chem. B* **2008**, *112*, 7778–7784.
5. Echenique, G. D. R.; Schmidt, R. R.; Freire, J. J.; Cifre, J. G. H.; de la Torre, J .G. A Multiscale Scheme for the Simulation of Conformational and Solution Properties of Different Dendrimer Molecules. *J. Am. Chem. Soc.* **2009**, *131*, 8548–8556.
6. Yi, X.; Shi, X.; Gao, H. Cellular Uptake of Elastic Nanoparticles. *Phys. Rev. Lett.* **2011**, *107*, 098101.
7. Hong, S.; Bielinska, A. U.; Mecke, A.; Kezsler, B.; Beals, J. L.; Shi, X.; Balogh, L.; Orr, B. G.; Baker, J. R.; Holl, M. M. B. Interaction of Poly(amidoamine) Dendrimers with Supported Lipid Bilayers and Cells: Hole Formation and the Relation to Transport. *Bioconjugate Chem.* **2004**, *15*, 774–782.
8. Mullen, D. G.; Holl, M. M. B. Heterogeneous Ligand-Nanoparticle Distributions: A Major Obstacle to Scientific Understanding and Commercial Translation. *Acc. Chem. Res.* **2011**, *44*, 1135–1145.
9. Kelly, C. V.; Leroueil, P. R.; Orr, B. G.; Holl, M. M. B.; Andricioaei, I. Poly(amidoamine) Dendrimers on Lipid Bilayers I: Free Energy and Conformation of Binding. *J. Phys. Chem. B.* **2008**, *112*, 9337–9345.
10. Ginzburg, V. V.; Balijepalli, S. Modeling the Thermodynamics of the Interaction of Nanoparticles with Cell Membranes. *Nano Lett.* **2007**, *7*, 3716–3722.
11. Tian, W. D.; Ma, Y. Q. Theoretical and Computational Studies of Dendrimers as Delivery Vectors. *Chem. Soc. Rev.* **2013**, *42*, 705–727.
12. Yan, L. T.; Yu, X. Enhanced Permeability of Charged Dendrimers across Tense Lipid Bilayer Membranes. *ACS Nano* **2009**, *3*, 2171–2176.
13. Yan, L. T.; Yu, X. Charged Dendrimers on Lipid Bilayer Membranes: Insight through Dissipative Particle Dynamics Simulations. *Macromolecules* **2009**, *42*, 6277–6283.
14. Groot, R. D.; Warren, P. B. Dissipative Particle Dynamics: Bridging the Gap between Atomistic and Mesoscopic Simulation. *J. Chem. Phys.* **1997**, *107*, 4423–4435.

15. Grafmüller, A.; Shillcock, J.; Lipowsky, R. Pathway of Membrane Fusion with Two Tension-Dependent Energy Barriers. *Phys. Rev. Lett.* **2007**, *98*, 218101.
16. Yang, K.; Ma, Y. Q. Computer Simulation of the Translocation of Nanoparticles with Different Shapes across a Lipid Bilayer. *Nat. Nanotechnol.* **2010**, *5*, 579–583.
17. Yue, T.; Li, S.; Zhang, X.; Wang, W. The Relationship between Membrane Curvature Generation and Clustering of Anchored Proteins: a Computer Simulation Study. *Soft Matter* **2010**, *6*, 6109–6118.
18. Sens, P.; Gov, N. Force Balance and Membrane Shedding at the Red-Blood-Cell Surface. *Phys. Rev. Lett.* **2007**, *98*, 018102.
19. Doherty, G. J.; McMahon, H. T. Mechanisms of Endocytosis. *Annu. Rev. Biochem.* **2009**, *78*, 857–902.
20. Galleta, B. J.; Cooper, J. A. Actin and Endocytosis: Mechanisms and Phylogeny. *Curr. Opin. Cell Biol.* **2009**, *21*, 20–27.
21. Kelly, C. V.; Liroff, M. G.; Triplett, L. D.; Leroueil, P. R.; Mullen, D. G.; Wallace, J. M.; Meshinchi, S.; Baker, J. R.; Orr, B. G.; Holl, M. M. B. Stoichiometry and Structure of Poly(amidoamine) Dendrimer-Lipid Complexes. *ACS Nano* **2009**, *3*, 1886–1896.
22. Rudnck, J.; Gaspari, G. The Asphericity of Random-Walks. *J. Phys. A* **1986**, *19*, L191–L193.
23. Gratton, S. E. A.; Ropp, P. A.; Pohlhaus, P. D.; Luft, J. C.; Madden, V. J.; Napier, M. E.; DeSimone, J. M. The Effect of Particle Design on Cellular Internalization Pathways. *Proc. Natl. Acad. Sci. U.S.A.* **2008**, *105*, 11613–11618.
24. Zhang, S.; Li, J.; Lykotrafitis, G.; Bao, G.; Suresh, S. Size-Dependent Endocytosis of Nanoparticles. *Adv. Mater.* **2009**, *21*, 419–424.
25. Gao, H.; Shi, W.; Freund, L. B. Mechanics of Receptor-Mediated Endocytosis. *Proc. Natl. Acad. Sci. U.S.A.* **2005**, *102*, 9469–9474.
26. Helfrich, W. Possible Chromatographic Effect of Liquid-Crystalline Permeation. *Z. Naturforsch.* **1973**, *C28*, 693–703.
27. Deserno, M. Elastic Deformation of a Fluid Membrane upon Colloid Binding. *Phys. Rev. E* **2004**, *69*, 031903.
28. Morris, C. E.; Homann, U. Cell Surface Area Regulation and Membrane Tension. *J. Membr. Biol.* **2001**, *179*, 79–102.
29. Tian, W. D.; Ma, Y. Q. pH-Responsive Dendrimers Interacting with Lipid Membranes. *Soft Matter* **2012**, *8*, 2627–2632.
30. Gurtovenko, A. A.; Anwar, J.; Vattulainen, I. Defect-Mediated Trafficking across Cell Membranes: Insights from in Silico Modeling. *Chem. Rev.* **2010**, *110*, 6077–6103.
31. Tieleman, D. P.; Leontiadou, H.; Mark, A. M.; Marrink, S. J. Simulation of Pore Formation in Lipid Bilayers by Mechanical Stress and Electric Fields. *J. Am. Chem. Soc.* **2003**, *125*, 6382–6383.
32. Shillcock, J. C.; Lipowsky, R. Equilibrium Structure and Lateral Stress Distribution of Amphiphilic Bilayers from Dissipative Particle Dynamics. *J. Chem. Phys.* **2002**, *117*, 5048–5061.
33. Groot, R. D. Electrostatic Interactions in Dissipative Particle Dynamics Simulation of Polyelectrolytes and Anionic Surfactants. *J. Chem. Phys.* **2003**, *115*, 11265–11277.
34. Vattulainen, I.; Karttunen, M.; Besold, G.; Polson, J. M. Integration Schemes for Dissipative Particle Dynamics Simulations: from Softly Interacting Systems towards Hybrid Models. *J. Chem. Phys.* **2002**, *116*, 3967–3979.
35. Smith, K. A.; Jasnow, D.; Balazs, A. C. Designing Synthetic Vesicles that Engulf Nanoparticles. *J. Chem. Phys.* **2007**, *127*, 084703.
36. Dasgupta, S.; Auth, T.; Gompper, G. Wrapping of Ellipsoidal Nano-Particles by Fluid Membranes. *Soft Matter* **2013**, *9*, 5473–5482.
37. Lipowsky, R. Budding of Membranes Induced by Intramembrane Domains. *J. Phys. II France* **1992**, *2*, 1825–1840.
38. Kreyszig, E. *Differential Geometry*; Dover Publications: Mineola, NY, 1991.
39. Noguchi, H.; Gompper, G. Dynamics of Vesicle Self-Assembly and Dissolution. *J. Chem. Phys.* **2006**, *125*, 164908.
40. Goetz, R.; Gompper, G.; Lipowsky, R. Mobility and Elasticity of Self-assembled Membranes. *Phys. Rev. Lett.* **1999**, *82*, 221–224.
41. Siegel, D. P. Energetics of Intermediates in Membrane Fusion: Comparison of Stalk and Inverted Micellar Intermediate Mechanisms. *Biophys. J.* **1993**, *65*, 2124–21.
42. Vacha, R.; Martinez-Veracoechea, F. J.; Frenkel, D. Intracellular Release of Endocytosed Nanoparticles upon a Change of Ligand-Receptor Interaction. *ACS Nano* **2012**, *6*, 10598–10605.
43. Wang, Z. J.; Frenkel, D. Pore Nucleation in Mechanically Stretched Bilayer Membranes. *J. Chem. Phys.* **2005**, *123*, 154701.
44. Tolpekina, T. V.; den Otter, W. K.; Briels, W. J. Simulations of Stable Pores in Membranes: System Size Dependence and Line Tension. *J. Chem. Phys.* **2004**, *121*, 8014.